Reports

A Local Time-Dependent Sverdrup Balance in the Eastern North Pacific Ocean

Abstract. *Direct observations of the dynamic balance between time-dependent winds and deep ocean currents are described for the eastern North Pacific Ocean at 42°N, 152°W. Currents from 150 to 4000 meters below the surface at frequencies from 0.01 to 0.1 cycle per day are significantly correlated with the wind stress curl derived from U.S. Navy operational wind fields. The horizontal currents are depth-independent below 300 meters, and they flow parallel to the potential vorticity gradient derived from the earth's rotation and the large-scale bottom topography. These characteristics are expected for such periodic motions with horizontal scales larger than 500 kilometers and represent a generalized Sverdrup balance between the atmospheric forcing and the oceanic response.*

PEARN P. NIILER
Scripps Institution of Oceanography, La Jolla, California 92093
CHESTER J. KOBLINSKY
NASA Goddard Space Flight Center, Greenbelt, Maryland 20771

Early in this century, oceanographers attempted to relate atmospheric forcing to the energetic long-time-period (days to years) currents in the ocean. Early investigators derived a mechanism for momentum transfer from the atmosphere into the surface layers (*1*). The divergence of this wind-driven surface flow causes a vertical motion near the bottom of the mixed layer, termed Ekman pumping, that forces the underlying ocean. Steady Ekman pumping is responsible for the general baroclinic pattern of large-scale ocean circulation (*2, 3*). Measurements of time-dependent, wind-driven deep ocean currents have only been possible in the last decade. These measurements are now possible because of improvements in the analysis of available marine wind observations and developments in current-measuring instruments. Thus far, however, only a few observations of time-dependent ocean currents have suggested any direct relation to the winds (*4, 5*). We report here direct observations of the dynamic balance between winds and deep ocean currents.

Recent theoretical models (*4, 6*) suggest that the time-dependent, depth-independent dynamics of the mid-latitude ocean forced by a realistic wind field are conveniently separated into three frequency ranges. (i) Between 0.1 cycle per day and the inertial frequency ($f = 2\Omega \sin\theta$, where Ω is the rotation frequency of the earth and θ is the local latitude), the response is evanescent horizontally and vertically from the forcing area. This response is localized and does not resonate any traveling ocean wave forms. For this response, correlations between the wind stress and the local subsurface currents are possible and have been observed (*5*). (ii) Between about 0.01 and 0.1 cycle per day, barotropic Rossby waves (*7*) are excited in the models through resonance. These waves radiate the vorticity input by the wind field throughout the ocean; their amplitude depends upon frictional drag in the ocean. In this Rossby wave band, correlations between the forcing function and the local ocean should be small and unobservable because of the broad wave-number bandwidth of the free waves. (iii) Below frequencies of about 0.01 cycle per day, the barotropic Sverdrup balance (*3*) dominates the vorticity dynamics. The models suggest that correlations between the curl of the wind stress and the subsurface currents that are parallel to the local potential vorticity gradient should be observable in this regime. The model-predicted amplitude of wind-driven currents is 1 to 3 cm sec^{-1}. In subtropical oceans, fluid instabilities or ocean eddies also produce deep currents of similar magnitude and the deep wind-driven response is difficult to determine.

To test these hypotheses about wind-driven deep ocean currents, observations were made of horizontal ocean currents at 42°N, 152°W (Fig. 1) from June 1982 through May 1983, at ocean depths of 80, 150, 300, 400, 600, 1000, and 3800 m. The eastern North Pacific is a region of relatively low eddy energy (*8*) and is subjected to vigorous atmospheric forcing. In 1982 and 1983, atmospheric forcing was enhanced in this region because of the southward shift and anomalous strengthening of the Aleutian low-pressure system. These conditions were associated with a strong El Niño–Southern Oscillation event (*9*).

Estimates of the surface wind fields, referenced to 19.5 m above the surface (Fig. 1), were obtained from the U.S. Navy Fleet Numerical Oceanography

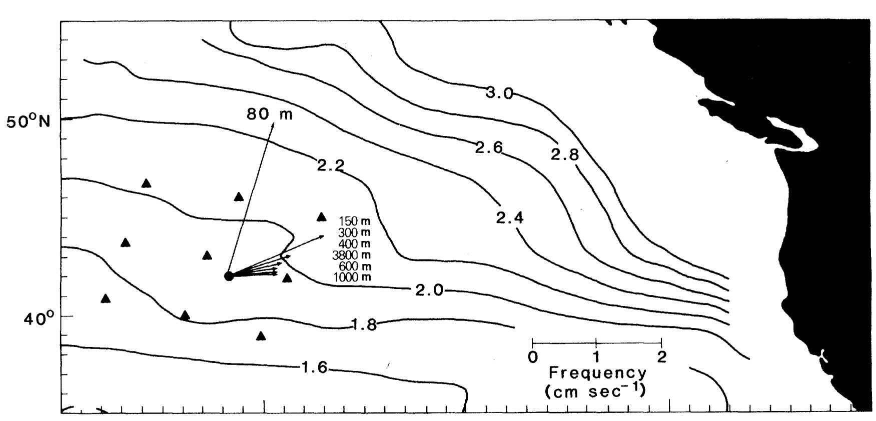

Fig. 1. The region of study in the eastern North Pacific Ocean. The site of the current meter mooring is marked by the large solid dot. The nearest Fleet Numerical Oceanography Center estimated winds were for the locations marked by triangles. The magnitude and orientation of the principal axis of the current meter variance ellipses are shown for various depths. Contours of the potential vorticity (f/h) are shown in units of 10^{-10} cm^{-1} sec^{-1}.

Center (*10*). The stress of the wind on the ocean surface was computed from the estimated wind fields (*11*). We computed the curl of the wind stress directly over the current meter mooring every 6 hours, using finite differences of a surface fitted (*12*) to the closest nine locations of the estimated wind stress. Both the wind and current data have been subjected to low-pass filtering to remove all variations with frequencies greater than 0.1 cycle per day and then a least-squares-fit cubic polynomial was used to remove a pronounced seasonal signal.

The potential vorticity of barotropic, geostrophic flow (*f*/*h*) has been computed (Fig. 1) from a 1° digitized bottom topography, *h* (*13*). The topography was smoothed to be consistent with the spatial scales resolved in the wind field. The slope of the topography is comparable to the fractional variation of the Coriolis parameter, so that the potential vorticity gradient is to the east-northeast.

In the frequency band from 0.01 to 0.1 cycle per day, the currents were depth-independent below 300 m (Fig. 2), especially in winter from day 280 to day 480, beginning on 1 January 1982. A weak baroclinic eddy field exists and decays with depth and is not coherent with winds. A number of fluctuations at 156 m on day 230 to day 320 are not replicated at 956 m, but the 606-m record has a high degree of correspondence with the 3756-m record (Fig. 2). Figure 1 displays the strength and orientation of the major axis of the current meter variance ellipse (*14*). The 600-, 1000-, and 3800-m records are parallel to the local gradient of barotropic potential vorticity.

The variance of the 80-m current is characterized by a north-south component. The mixed layer depth at 42°N, 152°W, varies seasonally from less than 50 m in summer to more than 100 m in winter (*15*); thus the 80-m current meter was within this layer from day 280 to day 480 where the wind-forcing was strong (*1, 16*). A complex linear regression analysis between the wind stress vector and the 80-m current vector for the winter time period reveals that this current vector magnitude is 37 ± 12 percent of the wind stress vector magnitude and is in phase with it, but at an angle of 78° ± 20° to the right of the wind stress with 95 percent confidence. These results are consistent with a slab model of the mixed layer (*16*) which extends deeper than 80-m during the winter.

The zonal wind stress is correlated with the currents below 100 m (Figs. 2 and 3). However, the currents precede the wind stress by a few days (Fig. 3). The lowest correlation is with the 156-m instrument. The curl of the wind stress is correlated with the subsurface zonal currents (Figs. 2 and 3). In this case, the forcing function (wind stress curl) leads the response (currents) by 1 to 2 days. The point where the curves cross zero, between 6 and 8 days, indicates that strongest relations have a monthly periodicity. The lag in correlation between the wind stress curl and the subsurface ocean currents suggests that this amount of time is required for the winds to establish the Ekman pumping. Theoretically, this lag should be one inertial period (18 hours), which, of course, is not well resolved by our filtering.

The dominant direction of the current fluctuations parallel to the potential vorticity gradient and their depth independence suggest a generalized Sverdrup balance. For a barotropic flow in the ocean, this balance is given by

$$\bar{u} \cdot \bar{\nabla}\left(\frac{f}{h}\right) = \frac{fk \cdot \bar{\nabla} \times \frac{\bar{\tau}}{\rho f}}{h^2} \qquad (1)$$

where $\bar{u}$ is the horizontal current vector, $\bar{\nabla}$ is the two-dimensional horizontal gradient operator, h is the local depth of the fluid, $\bar{\tau}(x,y)$ is the horizontal wind stress vector at the surface of the ocean, ρ is the mean density of the ocean, and k is the vertical unit normal. This balance indicates that vorticity imparted to the ocean by the atmosphere through the Ekman pumping mechanism must be compensated for by the advection of fluid columns across barotropic vorticity contours below the Ekman layer.

One can obtain a quantitative estimate of the balance implied by the potential vorticity equation (Eq. 1) on the basis of

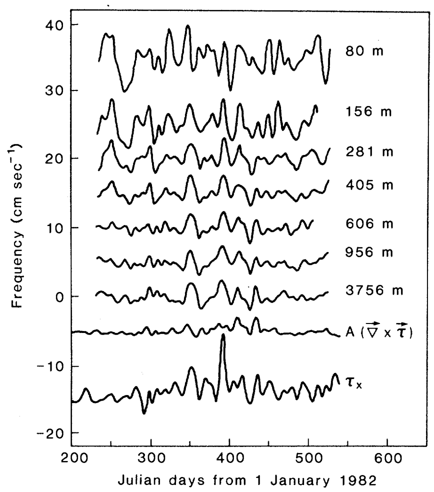

Fig. 2. The bandpassed zonal currents at various depths for 42°N, 152°W, during 1982 and 1983. All currents except those at 3800 m have been offset from a mean value of 0. The bandpassed zonal wind stress is shown as the bottom curve (in units of dynes per square centimeter); the wind stress curl, scaled by $A = (\beta h \rho^{-1})$ where β is the local north-south gradient of f (in units of centimeters per second), is the curve second from the bottom.

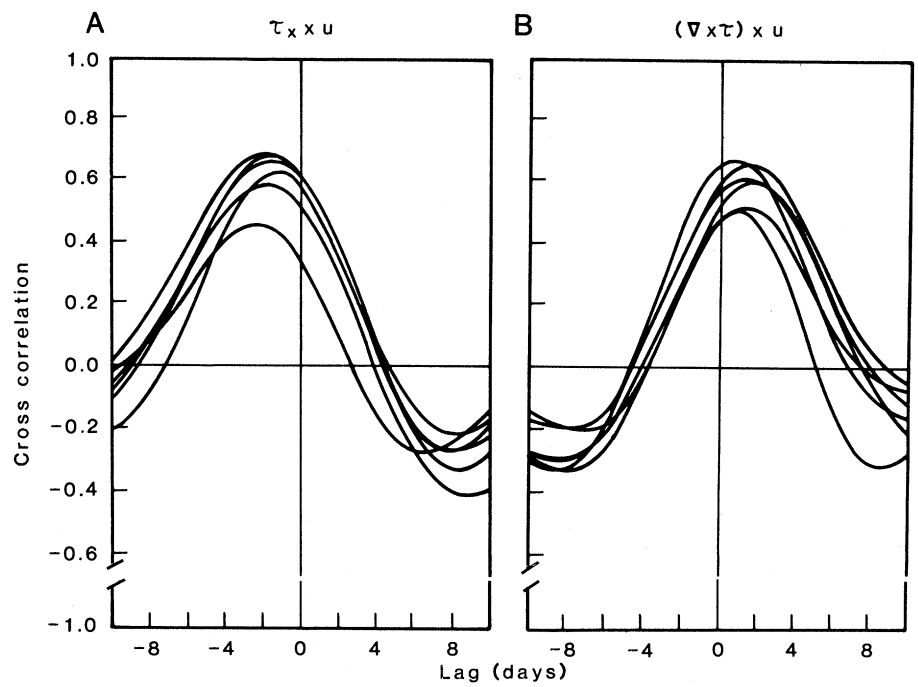

Fig. 3. (A) Correlations of the zonal wind stress and the zonal currents between day 280 and day 480 below 100 m. (B) Correlations of the wind stress curl and the zonal currents below 100 m. Near the zero lag, the curves with the smaller correlation values are for current meters that are closest to the surface in both (A) and (B). The zero hypothesis interval (95 percent confidence) from a parametric test (*18*) is ±0.43 for both (A) and (B); 90 percent nonparametric confidence intervals (*19*) have about the same width as the spread of the curves, which is ±0.1.

a linear regression of the right-hand side on the left-hand side. The 4000-m values of u and v between day 280 and day 480 are used with $\partial(f/h)/\partial x$ and $\partial(f/h)/\partial y$ as the unknowns determined from a least-squares fit. The left-hand side of Eq. 1 accounts for 60 percent of the variance of the right-hand side of Eq. 1, and the estimated bottom slopes are $\partial h/\partial x = 2.5 \pm 3.0 \times 10^{-4}$ and $\partial h/\partial y = -11.5 \pm 4.5 \times 10^{-4}$, with 95 percent confidence. From the digitized ocean topography, the respective values are estimated to be 4×10^{-4} and -13×10^{-4}. Hence, the wind-driven circulation is forced to flow zonally because of the Mendocino Escarpment.

These results are consistent with the time-dependent barotropic, linear vorticity equation provided that $(\omega/h\beta_e L) << 1$, where ω is the frequency of forcing, β_e is the equivalent potential vorticity gradient, and L is the scale of the wind stress (or bottom topography). Thus, for $\omega < 0.10$ cycle per day and $h\beta_e = 1.7 \times 10^{-11}$ $m^{-1}sec^{-1}$, motions with scales of $L \geq 450$ km are in Sverdrup balance. This scaling disagrees with the theoretical models (*4*), which suggest that Rossby waves are generated in this regime. There are two apparent reasons for this discrepancy. First, the wave-number spectrum of the winds for our observations could be quite different from the spectra used in those models. This would result in a scale mismatch between the atmosphere and the Rossby wave excitation band, leading to an inability of the atmosphere to excite the Rossby waves. Also, no specific theoretical computation has been made for the topographic regime of the eastern North Pacific. Second, a study of long-period tides (*17*) indicates that short-wavelength barotropic Rossby waves are dissipated much more quickly than had been assumed. Thus, any short-wavelength features would be rapidly damped and only the large-scale Sverdrup balance would remain.

Our results suggest that the northeastern Pacific Ocean has a much simpler dynamical response to atmospheric forcing at time periods from 10 to 100 days than has been argued. These measurements confirm that the ocean variability caused by atmospheric forcing is small compared with what results from fluid instabilities, such as those found in western boundary current regions.

References and Notes

1. V. W. Ekman, *Ark. Mat., Astron. Fys.* **2** (No. 11), 1 (1905).
2. H. Stommel, *Trans. Am. Geophys. Union* **29**, 202 (1948).
3. H. U. Sverdrup, *Proc. Natl. Acad. Sci. U.S.A.* **33**, 318 (1947).
4. P. Muller and C. Frankignoul, *J. Phys. Oceanog.* **11**, 287 (1981).
5. C. J. Koblinsky and P. P. Niiler, *ibid.* **12**, 144 (1982); R. R. Dickson *et al.*, *Nature (London)* **295**, 293 (1982).
6. S. G. H. Philander, *Rev. Geophys. Space Phys.* **16**, 15 (1978); C. Frankignoul and P. Muller, *J. Phys. Oceanog.* **9**, 104 (1979); J. Willebrand, S. G. H. Philander, R. C. Pacanowski, *ibid.* **10**, 411 (1980).
7. Rossby waves are the wave solutions of quasi-geostrophic dynamics and are discussed by J. Pedlosky [*Geophysical Fluid Dynamics* (Springer, New York, 1979)].
8. R. E. Cheney, J. G. Marsh, B. D. Beckley, *J. Geophys. Res.* **88**, 4343 (1983).
9. R. S. Quiroz, *Mon. Weather Rev.* **111**, 1685 (1983).
10. The Fleet Numerical Oceanography Center (Monterey, Calif.) forecasts wind fields for the mid-latitude Northern Hemisphere on a 2.5° polar stereographic grid (Fig. 1) by incorporating real time observations with a dynamical forecast model. C. A. Friehe and S. E. Pazan, *J. Appl. Meteorol.* **17**, 1488 (1978).
11. Wind stress has been computed with the standard bulk formula $\bar{\tau} = (\tau_x, \tau_y) = \rho_a C|\bar{u}_w|(u_w, v_w)$, where ρ_a is the air density near the surface of the ocean, C is the drag coefficient, and (u_w, v_w) are the east-west and north-south components of the wind vector. We have used a drag coefficient for a neutrally stable atmosphere which varies with wind speed [derived empirically by J. R. Garratt, *Mon. Weather Rev.* **105**, 915 (1977)].
12. H. Akima, *Assoc. Computer Mach. Trans. Math. Software* **4**, 148 (1978).
13. The digitized bottom topography was obtained from the U.S. Defense Mapping Agency.
14. If u, v, are the east-west, north-south components of the current vector and $<u'u'>$ is the mean removed variance, then $0.5 \tan^{-1}[2<u'v'>/(u'u'> - <v'v'>)]$ is the angle between the east-west axis and the major axis of the mean-removed variance ellipse. This angle is positive when drawn from the east axis to the principal axis in the counterclockwise sense.
15. S. Levitus, *Natl. Oceanic Atmos. Admin. Prof. Pap. 13* (1982), pp. 149–150.
16. R. E. Davis, R. de Szoeke, P. P. Niiler, *Deep-Sea Res.* **28A**, 1453 (1981).
17. D. Luther, personal communication.
18. F. Sciremammano, *J. Phys. Oceanog.* **9**, 1273 (1979).
19. B. Effron, *Soc. Ind. Appl. Math. Rev.* **21**, 460 (1979).

20. We thank S. Pazan and J. Bytoff for supplying the mid-latitude wind fields.

17 September 1984; accepted 10 June 1985

Anthropoid Origins in Asia? New Discovery of *Amphipithecus* from the Eocene of Burma

Abstract. *A new fossil of the primate* Amphipithecus mogaungensis *Colbert from the late Eocene of Burma shows that this species has a mandibular and molar morphology very similar to Oligocene and post-Oligocene higher primates. It has an exceptionally deep jaw. Its brachybunodont first and second molars have smooth enamel but lack hypoconulids. The shape of its second molar is nearly square—an advanced higher primate feature.* Amphipithecus mogaungensis *and related taxon* Pondaungia cotteri *Pilgrim are the earliest known higher primates. They suggest that Southeast Asia was an early theater of higher primate diversification.*

Russell L. Ciochon*
Institute of Human Origins, Berkeley, California 94709
Donald E. Savage
Department of Paleontology, University of California, Berkeley 94720
Thaw Tint
Department of Geology, Rangoon Arts and Sciences University, Rangoon, Burma
Ba Maw
Department of Geology, Mandalay Arts and Sciences University, Mandalay, Burma

*Current address: Department of Anatomical Sciences, State University of New York, Stony Brook 11794.

Amphipithecus mogaungensis Colbert was first described 48 years ago (*1*). Despite the recovery of only one partial jaw of the type, there has been continued debate about whether *Amphipithecus* was an anthropoid primate, as argued by Colbert (*1*) and later by Simons (*2*), or a lemuriform primate, possibly an adapid, as Szalay (*3*) and Szalay and Delson (*4*) concluded. Our discovery of another jaw fragment elucidates some aspects of this controversy.

The new jaw fragment (Department of Geology, Mandalay University, primate specimen DGMU-P1) was discovered in September 1978 by a Mandalay Arts and Sciences University field party during a survey in Burma's Pondaung Hills. It had weathered from claystone beds of the Pondaung Formation about 2.4 km west of Mogaung Village in northwestern central Burma near the site where Barnum Brown collected the type specimen of this species in 1923 (*1*). Other primate jaws (*5, 6*) and an associated vertebrate fauna have also been collected here and are currently being studied.

The Pondaung fauna (*7*) correlates with later Eocene Asian faunas from Yunnan, Gaungxi, Henan, Shaanxi, and Nei Mongol in China and with similar faunas in Mongolia (*8*). Correlation with faunas assigned to the Uintan and Duchesnean mammal ages in North America and to the late Robiacian and Headonian mammal ages in Europe is more tenuous. The overlying Yaw Formation, south of the Mogaung district, has been correlated with the Bartonian Age of Europe (*9*). Extended correlations with radiometrically dated rocks (*10*) indicate that the Pondaung fauna lived between 40 and 44 million years ago. Thus the